Toroidal varied line-space (TVLS) gratings

Roger J. Thomas

NASA's Goddard Space Flight Center, Laboratory for Astronomy and Solar Physics, Code 682, Greenbelt, MD 20771

ABSTRACT

It is a particular challenge to develop a stigmatic spectrograph for EUV wavelengths since the very low normal-incidence reflectance of standard materials most often requires that the design be restricted to a single optical element which must simultaneously provide both re-imaging and spectral dispersion. This problem has been solved in the past by the use of toroidal gratings with uniform line-space rulings (TULS). A number of solar EUV spectrographs have been based on such designs, including SOHO/CDS, Solar-B/EIS, and the sounding rockets SERTS and EUNIS. More recently, Kita, Harada, and collaborators have developed the theory of spherical gratings with varied line-space rulings (SVLS) operated at unity magnification, which have been flown on several astronomical satellite missions. These ideas are now combined into a spectrograph concept that considers varied-line space grooves ruled onto toroidal gratings. Such TVLS designs are found to provide excellent imaging even at very large spectrograph magnifications and beam-speeds, permitting extremely high-quality performance in remarkably compact instrument packages. Optical characteristics of two solar spectrographs based on this concept are described: SUMI, proposed as a sounding rocket experiment, and NEXUS, proposed for the Solar Dynamics Observatory mission.

Keywords: EUV, imaging spectrograph, toroidal grating, varied line-space, design

1. INTRODUCTION

It has been recognized for some time that the extreme ultraviolet (EUV) offers an extremely rich portion of the spectrum in which to carry out studies of the Sun's upper transition region and corona. Not only are there a wealth of strong EUV emission lines, but the plasma temperatures sampled by those lines are very well matched to the electron temperatures characteristic of emitting features found in the outer solar atmosphere, ranging between $2x10^4$ K and $2x10^7$ K. Furthermore, this wavelength regime contains a large number of line pairs that can be used as spectroscopic diagnostics to determine physical parameters directly, such as density and temperature for the plasma structures being observed. The atmospheric features themselves have considerable spatial complexity, with components on the order of 1 arcsec or less in width, but extending over lengths of several arcmin, as seen from the Earth. In addition, these features are now known to be highly dynamic, showing significant variations on time scales of a minute or less even under normal conditions, and much faster during periods of special activity such as flares, surges, or coronal mass ejections.

Thus, to obtain the maximum amount of information about such an emission source, the ideal solar EUV spectrograph must combine high spatial, spectral, and temporal resolutions with wide bandpass, large field of view and high sensitivity. And, because EUV observations can only be made above the Earth's absorbing atmospheric layers, the ideal instrument should also be as compact, light-weight, and rugged as practicable to withstand the rigors of space flight.

Early attempts to record imaged solar EUV spectra, such as the GSFC spectroheliograph[1] flown on OSO-7, relied entirely on grazing incidence optics for both the feeding telescope and the spectrograph's reflection grating, due to the very low normal-incidence reflectance of standard materials in the EUV. Unfortunately, those designs retain spatial resolution only for on-axis sources, and so observations of two-dimensional spatial areas had to be laboriously built up by scanning the instrument's small central field-of-view over the desired solar region point by point, taking as long as an hour to complete. The NRL spectroheliograph[2] flown on Skylab provided a major advance by using a single normal-incidence reflection from a concave objective grating, which simultaneously provided spatial re-imaging and spectral dispersion of the entire solar disk. Its major drawback was the fact that spatial and spectral information become completely entangled in one direction, producing so-called ‘overlappograph’ images of the Sun, so that full unambiguous interpretation is possible only for relatively isolated, compact, bright features in the solar atmosphere.

2. TOROIDAL UNIFORM LINE-SPACE (TULS) DESIGNS

Our SERTS sounding rocket payload[3] was the first to address these problems by using a telescope to feed an imaging normal-incidence EUV spectrograph consisting of a concave toroidal grating with uniform line-space rulings. The low efficiency of its single normal-incidence reflection is more than compensated for by its ability to record imaged spectra simultaneously from along the entire length of the spectrograph’s entrance slit. Furthermore, this class of design is capable of providing unambiguous measurements of spectral intensities, wavelength shifts, and line profiles for any type of EUV emitting feature anywhere on (or off) the solar disk. And the resulting spectrograph can indeed combine good spatial, spectral, and temporal resolutions over very useful wavelength ranges and spatial fields of view, and with adequate sensitivities. Following the success of our SERTS program, a number of other solar EUV spectrographs have been based on this design concept, including SOHO/CDS, Solar-B/EIS, and the future GSFC sounding rocket EUNIS.

The distances for horizontal and vertical focus (r_h, r_v) in a TULS spectrograph design are determined by five primary parameters: slit-grating distance (r_o), grating tilt (α), uniform ruling spacing (σ), and horizontal (R_h) and vertical (R_v) radii of curvature of the toroid, as follows:

$$r_h = \frac{R_h \cdot \cos^2\beta}{\cos\alpha + \cos\beta - R_h \cdot \cos^2\alpha / r_o} \tag{1}$$

$$r_v = \frac{R_v}{\cos\alpha + \cos\beta - R_v / r_o} \tag{2}$$

where dispersion angle (β) is related to spectral-order (m) times wavelength (λ) through the standard grating equation:

$$\sin\alpha + \sin\beta = m \cdot \lambda / \sigma \tag{3}$$

These five design parameters are adjusted to minimize the differences between horizontal and vertical focal-imaging surfaces over the desired spectral bandpass, thus providing quasi-stigmatic imaging over that range. The speed of the illuminating beam from the telescope is then set to give imaged spot sizes commensurate with the detector pixels to be used. Two other considerations are the spectral dispersion (given by a combination of ruling spacing and the spectrograph’s focal distance) and the spatial plate-scale (given by the telescope’s plate-scale times the spectrograph magnification, the latter of which is found from a ratio between the mean focal distance and r_o). These two scales are used to trade-off spectral resolution *vs*. bandpass on one hand, and spatial resolution *vs.* field of view on the other, in light of available detector area and pixel sizes.

3. SPHERICAL VARIED LINE-SPACE (SVLS) DESIGNS

More recently, Kita, Harada, and collaborators[4,5] have developed the theory of spherical varied line-space (SVLS) gratings, in which spacing varies from its nominal value (σ_o) as a function of distance (w) from the central groove. Although SVLS designs have only one grating-radius parameter (R), compared to the two for toroids, they use three more (b_2, b_3, and b_4) to describe the variations in line spacing of their straight grooves, as follows:

$$\frac{1}{\sigma} = \frac{1}{\sigma_o} \cdot \left(1 + \frac{2 \cdot b_2}{R} \cdot w + \frac{3 \cdot b_3}{R^2} \cdot w^2 + \frac{4 \cdot b_4}{R^3} \cdot w^3\right) \tag{4}$$

Harada *et al.*[5] have shown that these extra two parameters can be used to cancel exactly all on-axis astigmatic coma and spherical aberration, when the spectrograph is operating at a special condition near unity magnification. They also demonstrated that the SVLS is superior to an equivalent TULS system in terms of off-axis performance and insensitivity to optical misalignments under that special operating condition. Such designs have now been successfully used in several astronomical space missions, including the Berkeley Extreme Ultraviolet Spectrometer on the ORFEUS payload launched in 1993, and the Japanese Mid-Infrared Spectrometer on the IRTS satellite launched in 1995.

As with TULS spectrograph designs, the first five SVLS parameters (r_o, α, σ_o, R, b_2) are adjusted to minimize differences over the desired spectral bandpass between horizontal and vertical focal-imaging surfaces, as given by:

$$r_h = \frac{R \cdot \cos^2 \beta}{\cos\alpha + \cos\beta - R \cdot \cos^2 \alpha / r_o - 2 \cdot b_2 \cdot (\sin\alpha + \sin\beta)} \tag{5}$$

$$r_v = \frac{R}{\cos\alpha + \cos\beta - R/r_o} \tag{6}$$

where here the effective grating equation becomes:

$$\sin\alpha + \sin\beta = m \cdot \lambda / \sigma_o \tag{7}$$

Furthermore, the additional two parameters (b_3, b_4) are now available to control higher order aberrations after the focal conditions are set. However, in comparing these two classes of designs, the author has found that optimized SVLS systems tend to require significantly smaller values of grating tilt, α, than do the corresponding TULS cases. Since they both tend to operate best when close to the grating normal, this often means that fully optimized positions of the SVLS imaged spectrum may cause interference between incoming and outgoing light beams, thus making the aberration optimized design impractical, and requiring that some performance degradation be accepted. Another problem is that fully optimized SVLS imaging performance can actually be too good to be useful, in the sense that theoretical spot sizes may be far smaller than any available detector is able to record, even in principal. For such designs, the superior imaging quality of the SVLS grating is essentially wasted, since the over-all system performance is completely controlled by other factors. Those cases can always be improved, either in terms of better system resolution, larger collecting area, or more compact physical layout, by introducing higher magnification into the spectrograph design.

4. TOROIDAL VARIED LINE-SPACE (TVLS) DESIGNS

A logical extension of the concepts described above is to combine the two by considering gratings of varied line-space grooves ruled onto toroidal surfaces, allowing yet another design parameter with which to control imaging aberrations. In this case, Eq (7) remains valid as the effective grating equation, but the focal imaging distances are now given by:

$$r_h = \frac{R_h \cdot \cos^2 \beta}{\cos\alpha + \cos\beta - R_h \cdot \cos^2 \alpha / r_o - 2 \cdot b_2 \cdot (\sin\alpha + \sin\beta)} \tag{8}$$

$$r_v = \frac{R_v}{\cos\alpha + \cos\beta - R_v/r_o} \tag{9}$$

Ray-trace studies of such TVLS designs were first carried out though the author's personal code, which was modified by substituting the inverse of Eq (4) for the previously constant line spacing parameter, σ. These calculations were then validated by means of the commercial Interactive Ray-Trace (IRT) program, using a special module kindly provided by Webster Cash at the author's request. Finally, and again at the author's request, Focus Software Inc. was hired to write a special module for their general optics program, Zemax, to support this new class of spectrograph design. The resulting surface type, presently available only in the EE edition of Zemax, is named ‘Elliptical Grating’. This surface is invoked with eight parameters: central ruling frequency (T_o), diffraction order (m), three surface factors (a,b,c), and three ruling factors (A,B,Γ), which are related to the standard TVLS parameters as follows:

$$T_o = 1/\sigma_o \qquad \text{(but in units of lines per micron)} \tag{10}$$

$$a = 1/\sqrt{R_h \cdot R_v} \qquad b = 1/R_h \qquad c = R_h \tag{11}$$

$$\mathrm{A} = -2 \cdot b_2/(R_h \cdot T_o) \tag{12}$$

$$\mathrm{B} = (4 \cdot b_2^2 - 3 \cdot b_3)/(R_h^2 \cdot T_o) \tag{13}$$

$$\Gamma = 4 \cdot (-2 \cdot b_2^3 + 3 \cdot b_2 \cdot b_3 - b_4)/(R_h^3 \cdot T_o) \tag{14}$$

Analytic relations for the inverse conversions are then:

$$\sigma_o = 1/T_o \qquad R_h = c \qquad R_v = b/a^2 \tag{15}$$

$$b_2 = R_h \cdot T_o/2 \cdot \mathrm{A} \tag{16}$$

$$b_3 = R_h^2 \cdot T_o/3 \cdot (\mathrm{B} - \mathrm{A}^2 \cdot T_o) \tag{17}$$

$$b_4 = R_h^3 \cdot T_o/4 \cdot (\Gamma - 2 \cdot \mathrm{A} \cdot \mathrm{B} \cdot T_o + \mathrm{A}^3 \cdot T_o^2) \tag{18}$$

Ray-trace studies using all of these codes show that TVLS designs can provide excellent imaging even at very large spectrograph magnifications and beam-speeds, permitting extremely high-quality performance in remarkably compact instrument packages. Optical characteristics of two solar spectrographs based on this concept are described below.

4.1 Solar Ultraviolet Magnetograph Investigation (SUMI)

The SUMI instrument is a solar imaging polarimeter being proposed by NASA’s Marshall Space Flight Center under the leadership of Jason Porter as a sounding rocket payload. It is optimized to measure magnetic fields directly by means of polarization effects in the UV emission lines of C IV 1550 Å and Mg II 2800 Å, formed in the Sun’s transition region and upper chromosphere, respectively. The overall optical system includes a Ritchey-Chretien telescope, a retardation waveplate, and a beam-splitting Double Wollaston analyzer, all of which have been described previously by West *et al.*[6] In addition, to observe the magnetic signature of Zeeman splitting in the solar UV emission, an imaging spectrograph is required to provide the necessary wavelength resolution for the Stokes polarization analysis (Figure 1). Design of that spectrograph was particularly challenging, due to aberrations from the Double Wollaston analyzer, the very fast f/11.3 beam from the feeding telescope, the need to image two widely different wavelength sets simultaneously, and the physical limitations of a sounding rocket envelope. Furthermore, it was desirable to focus both polarization beams onto the same detector face for each wavelength set, and to do all this with a grating design requiring just one master ruling.

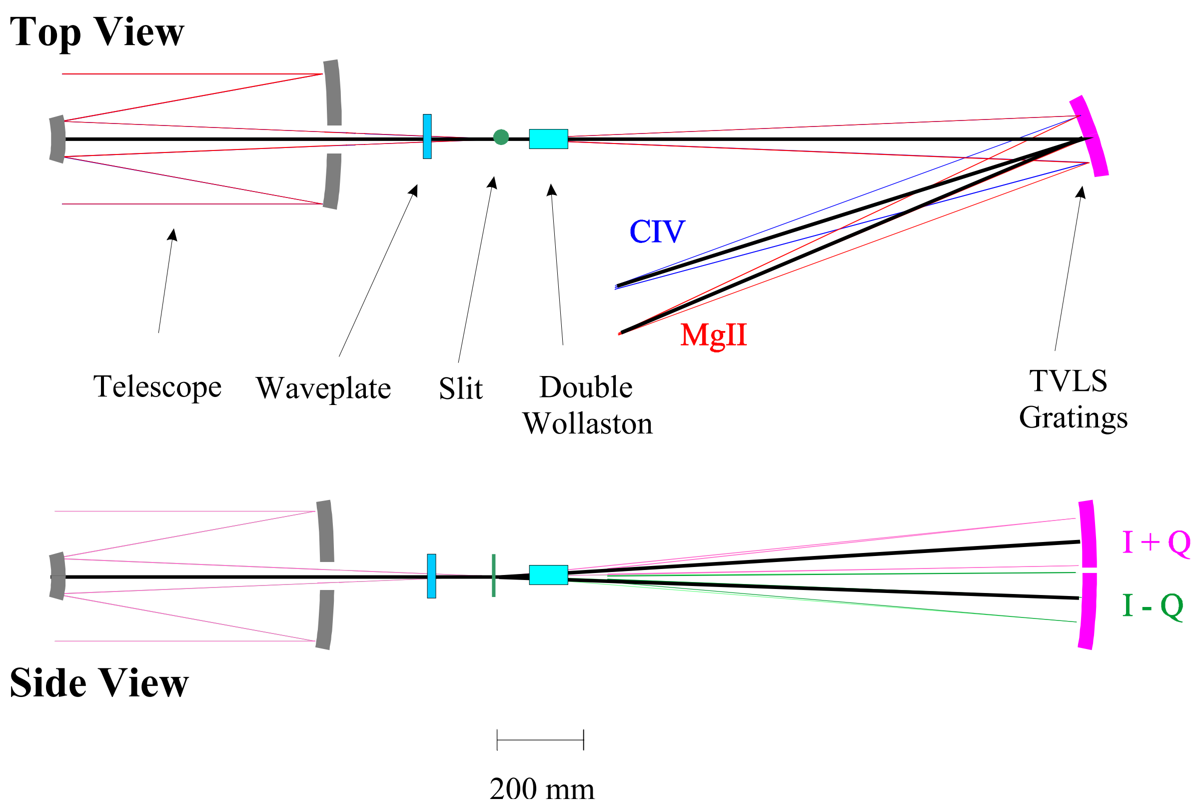

FIGURE 1. SUMI instrument concept. The top view shows the wavelength splitting of the gratings while bottom view shows the two output beams of the double Wollaston analyzer.

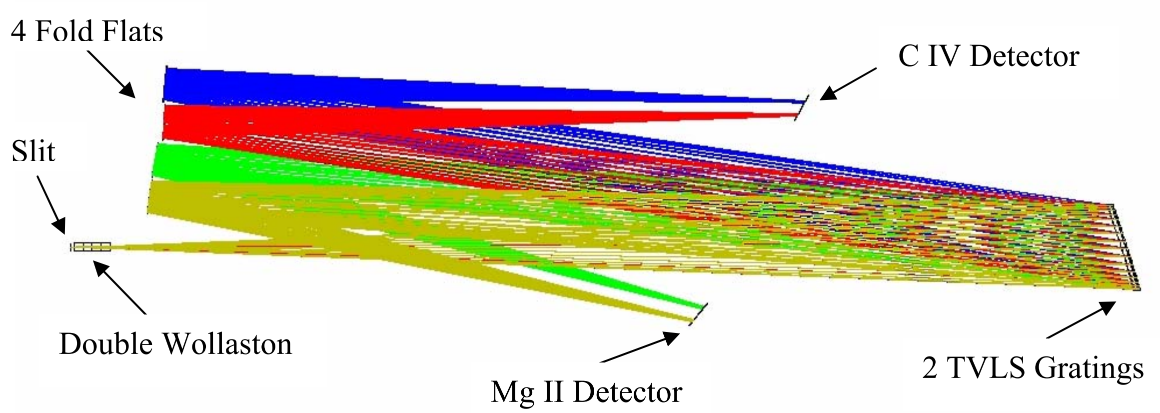

FIGURE 2. SUMI spectrograph layout as seen from above its dispersion plane. The side view is similar to that shown in Figure 1. Four fold-flats are individually positioned and tilted to redirect the four light beams onto a total of two different detectors.

The solution was found by combining two identical TVLS gratings, one for each polarization beam, with four flat folding mirrors to position the final focal points properly (Figure 2). Although the grating designs are the same, their tilts are independent and thus were optimized separately, as were the positions and tilts of each fold-flat and detector. To bring the dispersion directions of the two wavelength pairs closer together, C IV lines are observed in second spectral order, while Mg II lines are in first order. The final grating design parameters are: width = 124 mm, height = 142 mm, central ruling frequency = 2400 line/mm, R_h = 1500.000 mm, R_v = 1601.946 mm, blaze angle = 21.90°, b_2 = 0.233542, b_3 = 0.067279, and b_4 = 0.043365. The two copies of this grating are both placed at a total distance from the slit of r_o = 1444.000 mm, one above the other, but operated at the two different tilt angles of α = 17.093° and 18.170°, respectively.

The spectrometer design is matched to the two detectors currently chosen for SUMI: 256x1024 24 μm pixels for C IV, and 512x1024 13.5 μm pixels (in Frame-Transfer mode) for Mg II. It has the two polarization beams optimized onto a single focal plane for each line-pair, and all optical components are positioned to have clearance relative to each other and to all light-beams. The total optical width of the instrument, including the large telescope primary mirror, is 394 mm (15.5 inch), so that it will just fit within the standard sounding rocket skin of 17-inch diameter.

Ray-trace studies of the complete instrument show that its theoretical performance is remarkably good. The field averaged values of spatial and spectral resolutions are 1.40 arcsec and 24 mÅ for C IV, and 1.27 arcsec and 44 mÅ for Mg II (calculated by taking a Root-Sum-Square of the detector pixel size and twice the RMS-spot radius, converted by the appropriate spatial or spectral dispersion scale). These averages were taken over the desired full field of view of 142 arcsec, but the current detectors will actually cover FFOVs of 220 arcsec for C IV and 260 arcsec for Mg II, where performance is still excellent due to the impressive off-axis imaging properties of TVLS gratings.

4.2 Normal Incidence Extreme-Ultraviolet Imaging Spectrometer (NEXUS)

NEXUS has been proposed by the Naval Research Laboratory under the leadership of Kenneth Dere as the UV/EUV imaging spectrometer on the Solar Dynamics Observatory satellite mission. This design also was especially challenging due to the need for very high resolution imaging over the large spectral bandpass of 457 – 800 Å, with high throughput, and within the extremely tight physical volume and weight limits imposed by the allowable spacecraft resources. Once again, the solution turned out to involve a very fast feeding telescope and TVLS grating, but this time with a total of only two optical reflections being compensated with an enormous amount of magnification in the spectrograph (Figure 3).

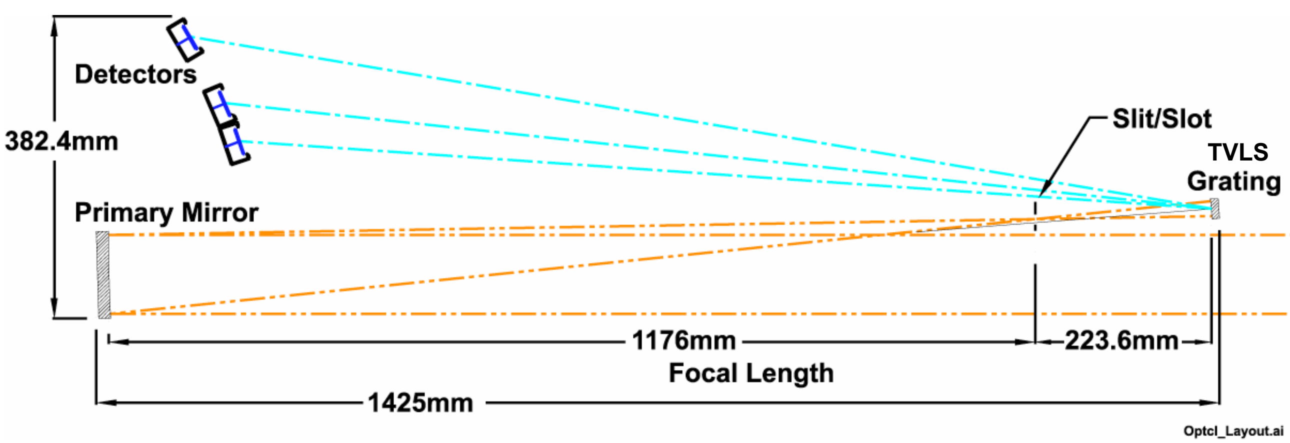

FIGURE 3. NEXUS optical layout as seen from above its dispersion plane. One TVLS grating feeds three individually positioned detectors to cover the instrument's broad spectral bandpass. Note the very large magnification in the spectrograph section, and the fact that optimized detector positions are very far off from the grating normal.

The NEXUS optical design consists of five components: an entrance aperture, telescope, slit, grating, and focal plane. Light admitted by the entrance aperture illuminates the off-axis parabolic telescope mirror, which forms a real solar image at the spectrometer's slit plane. The slit selects a portion of that solar image and passes it onto a concave diffraction grating, which then re-images it at the final focal plane simultaneously in each of the dispersed wavelengths. The stigmatic spectra thus produced have high spectral resolution in one dimension while maintaining high spatial resolution in the other. Moreover, large spectral bandpasses and spatial fields of view are covered instantaneously without need to move either the grating or detectors. This novel optical design was developed and optimized using Zemax, and verified by the personally written ray-trace code of the author. Some ray-trace results for this design, and an indication of its very large field of view, are shown in Figure 4. NEXUS technical design parameters are given at the top of the following page.

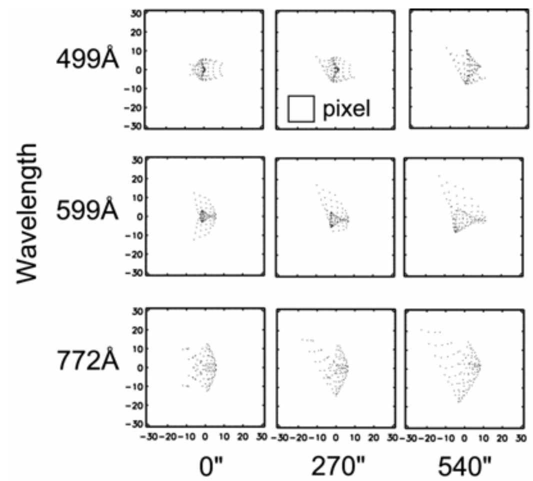

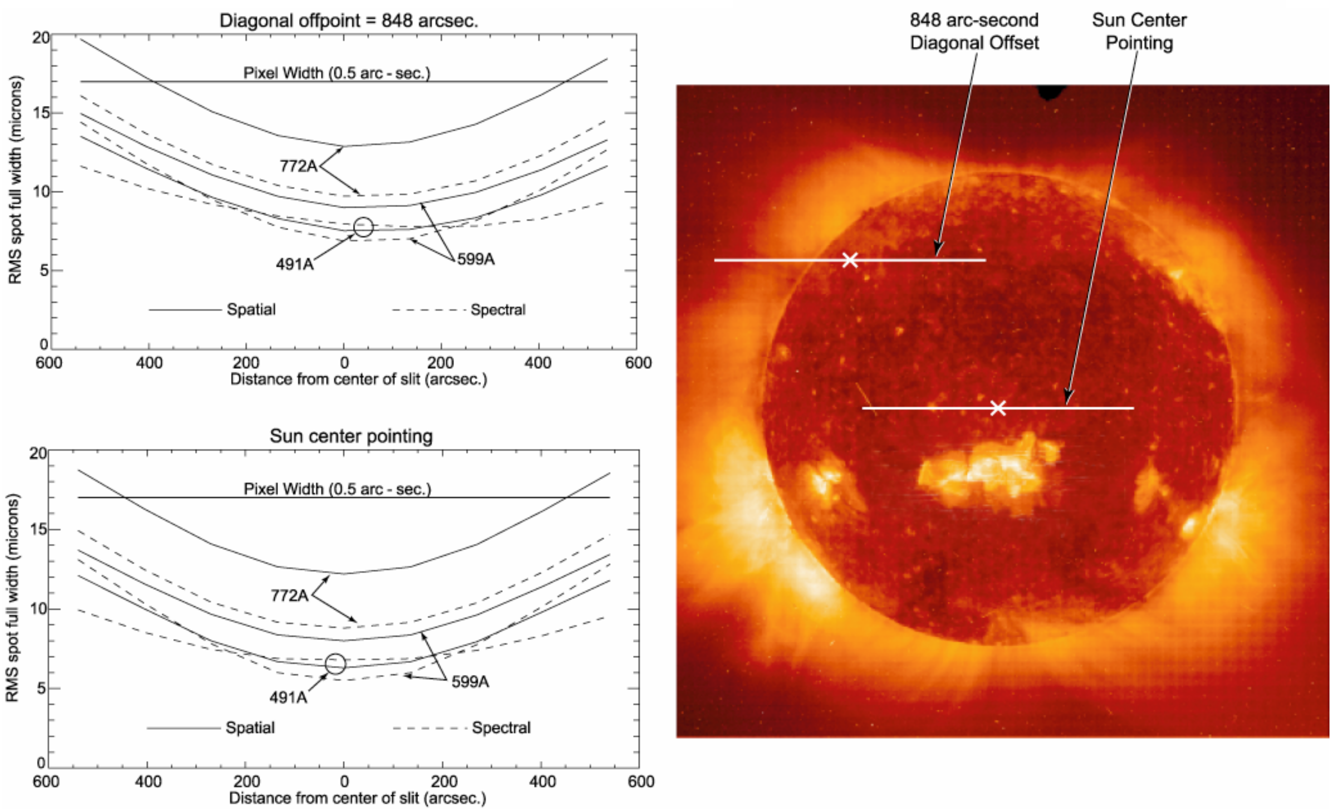

FIGURE 4. NEXUS ray-trace results and field of view. Spot diagrams are shown in the upper right, for wavelengths at the center of each detector, and at three field positions; the detector pixel size is also indicated for comparison. Curves of these results are shown at the left, for each of the two solar pointing fields of view as illustrated on the lower right.

Spectral bandpasses = 457-525 & 566-631 & 743-800 Å; Telescope dimensions = 108 x 102 mm (rectangular), vertex offset = 70 mm, (parabola) focal length = 1176 mm; Slit to grating distance = 224 mm; Total instrument optical envelope = 1400 x 368 x 108 mm; Slot/slit width = 342 / 3.0 µm (60 / 0.5 arcsec), length = 6.2 mm (1080 arcsec); Grating width = 21.0 mm, height = 25.0 mm, central ruling frequency = 3400 line/mm, R_h = 375.000 mm, R_v = 377.035 mm, α = -1.105°, blaze angle = 4.90°, b2 = 0.052859, b3 = 0.040301, b4 = 0.339541; Mid-Grating to focus distance = 1270.9 mm; Mid-Spectrometer magnification = 5.67; Average spectral dispersion = 1.934 Å/mm (32.9 mÅ/pix); Mid spatial plate scale = 32.3 µm/arcsec (0.526 arcsec/pix); Full spatial field of view = 18.0 arcmin.

The telescope is a single off-axis parabolic mirror, slightly larger than the instrument's entrance aperture to avoid vignetting over the full observed field of view. The mirror's surface is coated with an EUV multilayer tuned to the observed spectral bandpass for enhanced throughput. It is held by positioning mechanisms to permit active image-motion compensation, offset solar pointing, and focus corrections. Another mechanism will allow several slit options, all 6.2 mm in length to give a full 18 arcmin spatial field. The narrowest slit is 3.0 µm wide, for the highest spatial and spectral resolutions. These slits are fabricated from single crystal Silicon wafers using precision lithography techniques developed at GSFC and validated on several successful SERTS flights. There is also a 'slot' 342 µm wide which produces monochromatic images of high purity 60 x 1080 arcsec in size, allowing a rapid mosaic of the full solar disk to be made with NEXUS in many EUV lines covering a broad temperature range.

As mentioned above, the NEXUS grating is a toroidal varied line-space (TVLS) design, which provides excellent imaging even at very large spectrograph magnifications (x 5.7) and beam-speeds (f/11), permitting extremely high-quality performance within a remarkably compact instrument package. Despite its unique design, there should be no particular difficulty in ruling this TVLS grating for NEXUS, according to potential vendors. The grating surface itself is also coated with the same multilayer as the telescope, again to improve EUV reflectance.

Large spectrograph magnification has several advantages. Without resorting to folding mirrors that lose light, the NEXUS design most effectively uses all of the available instrument length, since the grating-detector leg closely matches the telescope-slit-grating length. Also, the grating-detector leg is as long as possible within the allowed instrument envelope, giving the highest spatial and spectral plate-scales. One power of the TVLS grating is that its optical aberrations are modest even under such extreme values of magnification, so that the achievable spatial and spectral resolutions are spectacular. With all of the instrument's magnification built into the spectrograph, the entire optical train is accomplished with only two reflecting surfaces, giving the highest possible EUV throughput. In addition, the TVLS grating can accommodate a very fast incoming optical beam, so that the telescope is extremely large for such a compact spectrometer, still further increasing the instrument's sensitivity.

The many advantages of TVLS designs make them very attractive candidates, indeed, for the next generation of solar EUV imaging spectrographs on future space missions.

REFERENCES

1. W.M. Neupert, R.J. Thomas, & R.D. Chapman, "Spatial Distribution of Soft X-Ray and EUV Emission Associated with a Chromospheric Flare of Importance 1B on August 2, 1972", Solar Physics **34**, 349-375, 1974.
2. R. Tousey, J.-D.F. Bartoe, G.E. Brueckner, & J.D. Purcell, "Extreme Ultraviolet Spectroheliograph: ATM Experiment S082A", Applied Optics **16**, 870-878, 1977.
3. W.M. Neupert, G.L. Epstein, R.J. Thomas, & W.T. Thompson, "An EUV Imaging Spectrograph for High-Resolution Observations of the Solar Corona", Solar Physics **137**, 87-104, 1992.
4. T. Kita & T. Harada, "Use of Aberration-Corrected Concave Gratings in Optical Demultiplexers", Applied Optics **22**, 819-825, 1983.
5. T. Harada, H. Sakuma, Y. Ikawa, T. Watanabe, and T. Kita, "Design of High-Resolution XUV Imaging Spectrometer using Spherical Varied Line-Space Grating", SPIE Proc**.** **2517**, 107-115, 1995.
6. E.A. West, J.G. Porter, J.M. Davis, G.A. Gary, D.M. Rabin, R.J. Thomas, & J.M. Davila, "Overview of the Solar Ultraviolet Magnetograph Investigation", Proceedings SPIE **4139**, 350-361 (2000).